Digital Signal Processing 48 (2016) 93–103

Contents lists available at ScienceDirect

Digital Signal Processing

www.elsevier.com/locate/dsp

Robust unscented Kalman filter with adaptation of process and measurement noise covariances

Wenling Li [a,*], Shihao Sun [a], Yingmin Jia [a], Junping Du [b]

[a] The Seventh Research Division, Beihang University (BUAA), Beijing 100191, China
[b] Beijing Key Laboratory of Intelligent Telecommunications Software and Multimedia, School of Computer Science and Technology, Beijing University of Posts and Telecommunications, Beijing 100876, China

ARTICLE INFO

Article history:
Available online 28 September 2015

Keywords:
Adaptation
Unscented Kalman filter
Masreliez–Martin filter
Relative navigation
Robot arm tracking

ABSTRACT

Unscented Kalman filter (UKF) has been extensively used for state estimation of nonlinear stochastic systems, which suffers from performance degradation and even divergence when the noise distribution used in the UKF and the truth in a real system are mismatched. For state estimation of nonlinear stochastic systems with non-Gaussian measurement noise, the Masreliez–Martin extended Kalman filter (EKF) gives better state estimates in relation to the standard EKF. However, the process noise and the measurement noise covariance matrices should be known, which is impractical in applications. This paper presents a robust Masreliez–Martin UKF which can provide reliable state estimates in the presence of both unknown process noise and measurement noise covariance matrices. Two numerical examples involving relative navigation of spacecrafts demonstrate that the proposed filter can provide improved state estimation performance over existing robust filtering approaches. Vision-aided robot arm tracking experiments are also provided to show the effectiveness of the proposed approach.

1. Introduction

Kalman filter has been one of the most popular state estimation techniques for linear stochastic systems. This is partly due to its wide range of applications in industrial areas such as target tracking, spacecraft navigation and signal processing [1,2]. One main concern for Kalman filter is that it requires an accurate system model and exact noise statistics information. These limitations, however, are too strong to be always satisfied in real applications. The lack of exact information may induce large state estimation errors and even filter divergence. To overcome this problem, a number of robust filters have been proposed to mitigate the impact of the inaccurate information [3–17]. Typically, two strategies can be used to address the filtering problem with unknown noise statistics including estimating the noise statistics [8,10,14–16] and ignoring the noise statistics [13]. Although the H_∞ filter can guarantee bounded state estimation error, it can in fact be worse than those generated by the Kalman filter in a least-squares sense. The adaptation of noise covariances has been an important topic for developing robust Kalman filters. One of the methods for adaptation is to use a scale or a matrix factor as a multiplier to the process or measurement noise covariance matrices so that the adaptation against both the system uncertainty and the measurement malfunctions is possible.

For state estimation of nonlinear stochastic systems, extensions and generalizations have been proposed such as the robust extended Kalman filter (EKF) [18–21] and the Huber-based divided-difference filter [22,23]. In [18], the Masreliez–Martin method was used to develop a robust EKF in the case when the process noise has a Gaussian distribution and the measurement noise has a non-Gaussian distribution. In [19], an adaptive fading EKF was proposed by introducing a forgetting factor in the gain matrix. In [20], a robust EKF is proposed for the attitude estimation of small satellite. A forgetting factor is adopted in the gain matrix to compensate measurement uncertainties and faults. These results are extended to develop a robust EKF by using a matrix forgetting factor in [21]. Simulations results in [18–21] show that robust filters outperform the standard EKF when the noise covariances used in the robust filters and the truth are mismatched. Although it is straightforward and simple to develop robust EKF, the EKF suffers from its own drawbacks such as instability due to linearization and costly calculation of Jacobian matrices. Another alternative for state estimation of nonlinear stochastic systems is the particle filtering approach [24–28]. In [24], the particle Markov Chain Monte Calro (PMCMC) method has been developed for nonlinear non-Gaussian systems with unknown static parameters, which are MCMC algo-

* Corresponding author.
E-mail addresses: lwlmath@buaa.edu.cn (W. Li), jxcrssh@126.com (S. Sun), ymjia@buaa.edu.cn (Y. Jia), junpingdu@126.com (J. Du).

http://dx.doi.org/10.1016/j.dsp.2015.09.004
1051-2004/

rithms that use a particle filter as a proposal mechanism. In [25], particle filter and smoother have been proposed for nonlinear systems by incorporating sequential parameter learning strategy. The key assumption for the proposed filter and smoother is the existence of a conditional sufficient statistic structure for the parameters. In [26], a generic approach has been developed called the sequential Monte Carlo (SMC^2) method. It should be pointed out that the SMC^2 is a sequential but not an on-line algorithm and the computational load increases with iterations owing to the associated cost of the MCMC steps. Nevertheless, the SMC^2 may offer several advantages over PMCMC in batch estimation scenarios [26]. In [27], nested particle filters have been proposed to approximate the posterior probability measure of the static parameters and the dynamic state variables of the system of interest. Unlike the SMC^2 scheme, the nested particle filters operate in a recursive manner and the computational complexity of the recursive steps is constant over time. In [28], the similarities and differences among the multiple try Metropolis (MTM) schemes and the particle Metropolis-Hastings (PMH) method have been investigated.

As stated in [29], it is easier to approximate a probability distribution than to approximate an arbitrary nonlinear transformation, the unscented Kalman filter (UKF) has been proposed for state estimation of nonlinear stochastic systems [29]. The main advantage of the UKF is that it does not use any linearization for calculating the state predictions and covariances. Many robust UKF variants have been proposed [30–40]. For instance, the H_∞ performance criterion has been combined with the UKF to improve the robustness against model errors and noise uncertainty in [30]. However, it is difficult to determine the performance level and the weighting matrices. In [31–34], several robust UKF algorithms have been proposed for nonlinear stochastic systems with measurement malfunctions. An adaptation scheme with multiple scale factors is used for adapting the measurement noise covariances so that only the data of the faulty sensor is scaled and any unnecessary information loss is prevented. Their applications in small satellite attitude estimation show that the fault can be detected accurately and the estimation performance can be improved greatly. In [35], the moving windowing approach is applied to develop an adaptive UKF where the historical innovation sequences are used to evaluate the measurement noise covariance. Simulation results show that the adaptive UKF outperforms the standard UKF when the precise knowledge of measurement noise statistics is unknown. It is shown that the performance can be further improved by estimating the measurement noise covariance using the present innovation [36]. It should be pointed out all the aforementioned work focus on adaptation of measurement noise covariance and the process noise parameters are not estimated. As a result they may be susceptible to unmodeled errors in the state propagation.

The case of unknown process noise covariance is often encountered in maneuvering target tracking and navigation systems [4], large state prediction errors may occur if the process noise covariance is not designed correctly. To this end, adaptation strategies have been proposed for process noise covariance in the UKF. For example, the robust UKF was developed for system fault detection in [37–39], where an adaptation scheme is carried out to detect the system fault. The application in nanosatellites attitude estimation shows that the robust UKF is fault tolerant against the sensor malfunctions. In [40], the fading factor is adopted to reduce the effect of the dynamics model errors and a robust estimation strategy is introduced to suppress the measurement model errors. Although the effect of the dynamic model error and the measurement error can be reduced simultaneously, the process and the measurement noise should be Gaussian distributions with known covariance matrices [37–40].

In this paper, we attempt to propose a robust UKF for nonlinear stochastic systems with Gaussian process noise and non-Gaussian measurement noise. The Masreliez–Martin EKF has been developed for such systems [18]. However, the process noise and the measurement noise covariance matrices should be known. To improve the estimation performance and practical usefulness, this paper aim to propose a robust UKF with adaptation of the process and the measurement noise covariance matrices. The fading factor is adopted to adjust the pre-designed process noise covariance and the innovation sequences are used to evaluate the measurement noise covariance. The simulation results are provided via relative navigation of spacecrafts. Experiments are also presented to evaluate the effectiveness of the adaptation strategies.

The rest of this paper is organized as follows. The problem of state estimation for nonlinear stochastic systems is formulated in Section 2. In Section 3, adaptation strategies are provided to estimate the process noise and measurement noise covariance matrices, which are used to develop a robust Masreliez–Martin UKF. In Section 4, two numerical examples are provided to illustrate the effectiveness of the proposed filter. In Section 5, experiments involving robot arm tracking are provided to show the effectiveness of the proposed adaptation strategies. Conclusion is drawn in Section 6.

2. Problem formulation

2.1. Problem formulation

Consider the following discrete-time nonlinear stochastic system

$$x_k = f(x_{k-1}) + w_{k-1} \tag{1}$$

$$z_k = h(x_k) + v_k \tag{2}$$

where $x_k \in \mathbb{R}^n$ and $z_k \in \mathbb{R}^m$ are the system state and the measurement vectors at time step k, respectively. f and h denote the system transition function and the measurement function, respectively. The process noise w_{k-1} is zero-mean white Gaussian with covariance matrix Q_{k-1} and the measurement noise v_k is represented by

$$p(v_k) = (1-\varepsilon)p_N(v_k) + \varepsilon q(v_k) \tag{3}$$

where $p(v_k)$ denotes the probability density function of v_k. $p_N(v_k)$ is the nominal Gaussian density function $\mathcal{N}(v_k, 0, R_{k,1})$ and $q(v_k)$ is the contaminating probability density $\mathcal{N}(v_k, 0, R_{k,2})$. The parameter $\varepsilon \in (0, 1)$ is called the degree of contamination.

The Masreliez–Martin EKF has been developed for nonlinear stochastic systems in the case when the process noise has a Gaussian distribution, and the measurement noise has a non-Gaussian distribution [18]. It should be pointed out that the process noise covariance Q_{k-1} and the nominal measurement noise covariance matrix $R_{k,1}$ are assumed to be known in the Masreliez–Martin EKF. However, the noise covariance matrices Q_{k-1}, $R_{k,1}$ and $R_{k,2}$ are generally unknown accurately in real world applications. Moreover, it is known that the UKF has been shown to generally perform better than the EKF and the UKF provides a derivative-free alternative to the EKF in the framework of Bayesian estimation.

To improve the performance and practical value of the robust Masreliez–Martin EKF, the aim of this paper is to develop a modified Masreliez–Martin UKF for the discrete-time nonlinear stochastic system (1)–(2) with unknown noise covariance matrices.

2.2. Background

For state estimation of nonlinear systems with Gaussian noise, Julier and Uhlmann presented a novel filter called the UKF in [29]. Unlike the EKF which approximates the nonlinear state and measurement equations using linearization, a set of carefully chosen

Algorithm 1: The unscented transform [29].

Step 1. Generate $2n+1$ weighted sigma points based on the mean $\bar{x}$ and covariance P_x

$$\chi_0 = \bar{x}, \quad w_0 = \frac{\kappa}{n+\kappa}$$

$$\chi_s = \bar{x} + (\sqrt{(n+\kappa)P_x})_s, \quad w_s = \frac{1}{n+\kappa}, \quad s = 1, \cdots, n$$

$$\chi_s = \bar{x} - (\sqrt{(n+\kappa)P_x})_s, \quad w_s = \frac{1}{n+\kappa}, \quad s = n+1, \cdots, 2n$$

Step 2. Propagate sigma points and compute the estimated mean $\bar{y}$ and covariance P_y

$$\tau_s = f(\chi_s)$$

$$\bar{y} = \sum_{s=0} w_s \tau_s$$

$$P_y = \sum_{s=0} w_s (\tau_s - \bar{y})(\tau_s - \bar{y})^T$$

sigma points are used to represent the state distribution. These sigma points can completely capture the true mean and covariance of the Gaussian random variable. Moreover, the propagated sigma points through the nonlinear systems can capture the posterior mean and covariance accurately to the 3rd-order Taylor series expansion for any nonlinearity. Besides its higher approximation accuracy, this approach can avoid the cumbersome evaluation of Jacobian and Hessian matrices, making the algorithm easier to implement. The UKF has proven to be far superior to standard EKF in a wide range of applications such as passive target tracking and autonomous satellite navigation. Despite its recent popularity, the process noise and the measurement noise statistics should be known a prior in the UKF. To illustrate the basic idea of the UKF, the unscented transform is briefly reviewed. Let x be an n-dimensional random variable with mean $\bar{x}$ and covariance P_x. A second random variable y is related to x through the nonlinear transformation $y = f(x)$, the objective is to calculate the mean $\bar{y}$ and covariance P_y. The unscented transform is shown in Algorithm 1.

We provide a simple example to show that the unscented transformation keeps invariant for the first and the second central moments: considering $x \sim \mathcal{N}(0_2, I_2)$ and $y = x^T x$, the theoretical results for the random variable y are $\bar{y} = 2$ and $P_y = 4$. By using the unscented transform, the sigma points $\{\chi_s\}$ are given by $\{(0,0)^T, (\pm\sqrt{3}, 0)^T, (0, \pm\sqrt{3})^T\}$ and the weights are $\{1/3, 1/6, 1/6, 1/6, 1/6\}$. The propagated sigma points can be derived as $\{0, 3, 3, 3, 3\}$. Then the estimated mean and covariance can be derived as 2 and 4, respectively. It can be seen that the unscented transformation keeps invariant for the first and the second central moments.

The Masreliez–Martin Kalman filter has been developed for state estimation of linear systems with non-Gaussian measurement noise in [3]. To be more specific, the non-Gaussian measurement noise is represented as a mixture of nominal Gaussian distribution and contaminating Gaussian distribution. The game theory is used to develop the Masreliez–Martin Kalman filter by optimizing against the contaminating Gaussian distribution in the minmax sense. In other words, the Masreliez–Martin Kalman filter is robust against the contaminating Gaussian distribution and only the covariance matrix of the nominal Gaussian distribution is used for the implementation of the Masreliez–Martin Kalman filter. To address the filtering problem of nonlinear systems with non-Gaussian noise, Stojanovic and Nedic have proposed the Masreliez–Martin EKF in [18], which can be considered as an extension of the Masreliez–Martin Kalman filter. The main difference between the Masreliez–Martin EKF and the standard EKF is that the posteriori

Algorithm 2: The Masreliez–Martin EKF [18].

Given the state estimates $\hat{x}_{1|0}$ and its associated error covariance $P_{1|0}$ at time $k = 0$. Compute the state estimate at every time k as follows.

$$\hat{x}_{k|k-1} = f(\hat{x}_{k-1|k-1})$$

$$P_{k|k-1} = F_{k-1} P_{k-1|k-1} F_{k-1}^T + Q_{k-1}$$

$$T_k = (H_k P_{k|k-1} H_k^T + R_{k,1})^{-1/2}$$

$$K_k = P_{k|k-1} H_k^T T_k^T$$

$$\nu_k = T_k (z_k - h(\hat{x}_{k|k-1}))$$

$$\hat{x}_{k|k} = \hat{x}_{k|k-1} + K_k \Psi(\nu_k)$$

$$P_{k|k} = P_{k|k-1} - (1-\varepsilon) K_k \Psi'(\nu_k) K_k^T$$

$$\Psi(\nu_k) = [\psi(\nu_{k,1}), \cdots, \psi(\nu_{k,m})]^T$$

$$\Psi'(\nu_k) = \begin{bmatrix} \psi'(\nu_{k,1}) \cdots 0 \\ 0 \ddots 0 \\ 0 \quad \cdots \psi'(\nu_{k,m}) \end{bmatrix}$$

where the $\psi(\cdot)$ is the Huber function and

$$F_{k-1} = \frac{\partial f}{\partial x}\Big|_{\hat{x}_{k-1|k-1}}, \quad H_k = \frac{\partial h}{\partial x}\Big|_{\hat{x}_{k|k-1}}$$

covariance matrix is modified by using a Huber's function. It is shown that the Masreliez–Martin EKF has small sensitivity to the presence of outliers in comparison with the standard EKF. However, the evaluation of the Jacobian matrix is needed since the EKF is adopted. Moreover, the covariance noise matrix should be known a prior for the implementation of the Masreliez–Martin EKF. For completeness, the Masreliez–Martin EKF developed in [18] for (1)–(2) is shown in Algorithm 2.

3. Modified Masreliez–Martin UKF

In this section, an adaptation strategy is provided to develop a modified Masreliez–Martin UKF. To derive the state estimate of the discrete-time nonlinear stochastic system (1)–(2), the recursive solution to the Bayesian filter consists of two steps: prediction and update. We first present the update step with adaptively adjusting the measurement noise covariance. Then we propose an adaptive strategy for the process noise covariance to derive the predicted state estimate.

3.1. Update with adaptation of the measurement noise covariance

Assume that the predicted state estimate $\hat{x}_{k|k-1}$ and its corresponding covariance $P_{k|k-1}$ have been obtained at time step $k-1$, the predicted measurement and the innovation covariance matrices can be derived by using the unscented transform technique

$$\hat{z}_{k|k-1} = \sum_{s=0}^{2n} \omega_s h(\chi_{k|k-1}^s) \tag{4}$$

$$P_{k|k-1}^{xz} = \sum_{s=0}^{2n} \omega_s [\chi_{k|k-1}^s - \hat{x}_{k|k-1}][\chi_{k|k-1}^s - \hat{x}_{k|k-1}]^T \tag{5}$$

$$P_{k|k-1}^{zz} = \sum_{s=0}^{2n} \omega_s [h(\chi_{k|k-1}^s) - \hat{z}_{k|k-1}][h(\chi_{k|k-1}^s) - \hat{z}_{k|k-1}] \tag{6}$$

$$P_{k|k-1}^{ee} = P_{k|k-1}^{zz} + \hat{R}_k \tag{7}$$

where the weights ω_s and the sigma points χ_k^s are given by

$$\chi^0_{k|k-1} = \hat{x}_{k|k-1},\ \omega_0 = \frac{\kappa}{n+\kappa} \tag{8}$$

$$\chi^s_{k|k-1} = \hat{x}_{k|k-1} + (\sqrt{(n+\kappa)P_{k|k-1}})_s,$$

$$\omega_s = \frac{1}{2(n+\kappa)},\ s = 1, \cdots, n \tag{9}$$

$$\chi^{s+n}_{k|k-1} = \hat{x}_{k|k-1} - (\sqrt{(n+\kappa)P_{k|k-1}})_s,$$

$$\omega_s = \frac{1}{2(n+\kappa)},\ s = 1, \cdots, n \tag{10}$$

with κ being a scaling factor. The vector $(\sqrt{(n+\kappa)P_{k|k-1}})_s$ denotes either the s-th row or the s-th column of the matrix square root of $(n+\kappa)P_{k|k-1}$. In general, if the matrix square root A of P is of the form $P = A^T A$ then the sigma points are formed from the rows of A. Otherwise, the column of A are used if $P = AA^T$ [29].

Assume that the innovations are stationary, the innovation matrix can be also approximated by using innovations in a width of the moving window

$$P^{ee}_{k|k-1} = \frac{1}{N}\sum_{j=0}^{N-1} e_{k-j}e^T_{k-j} \tag{11}$$

where N is the width of the moving window. It should be pointed out that too large a window width suffers from the severe computational inefficiency and too small a window width might lead to large variance. Thus, it is important to choose a reasonable window width. As stated in [41], there are mainly two categories for choosing the window width: deterministic and stochastic. In the deterministic approach a cost function is usually defined within limited memory then optimization technique is used. For the stochastic framework, the window width is determined by minimizing variance parameters. In this paper, we do not focus on the window width and interested readers are referred to [41].

The innovation e_{k-j} is

$$e_{k-j} = z_k - \hat{z}_{k-j|k-j-1} \tag{12}$$

By comparing (7) and (11), an estimate of the matrix R_k can be given by

$$\hat{R}^\star_k = \frac{1}{N}\sum_{j=0}^{N-1} e_{k-j}e^T_{k-j} - P^{zz}_{k|k-1} \tag{13}$$

Notice that only the covariance matrix $R_{k,1}$ is estimated in the proposed filter. This is due to the fact that the covariance matrix $R_{k,2}$ of the contaminated Gaussian distribution is not used in the Masreliez–Martin filter. It should be pointed out that the estimated matrix $\hat{R}_k$ might be not diagonal and positive definite in the above computations. To avoid such situation, the following rule is suggested

$$\hat{R}_k = \mathrm{diag}\{|\hat{R}^\star_k(1)|, |\hat{R}^\star_k(2)|, \cdots, |\hat{R}^\star_k(m)|\} \tag{14}$$

where $\hat{R}^\star_k(s)$ is the s-th diagonal element of the matrix $\hat{R}^\star_k$. It can be seen that the proposed strategy (14) is suitable to address the filtering problem with a diagonal covariance matrix. Especially, the positive definiteness can be guaranteed by taking the absolute value of the estimates.

By using the Masreliez–Martin method, the updated state estimate can be derived by

$$\hat{x}_{k|k} = \hat{x}_{k|k-1} + K_k\Psi(\nu_k) \tag{15}$$

$$P_{k|k} = P_{k|k-1} - K_k\Psi'(\nu_k)K^T_k \tag{16}$$

where

$$\nu_k = [P^{ee}_{k|k-1}]^{-1/2}e_k \tag{17}$$

$$K_k = P^{xz}_{k|k-1}[P^{ee}_{k|k-1}]^{-T/2} \tag{18}$$

$$\Psi(\nu_k) = \left[\psi(\nu^1_k)\cdots\psi(\nu^m_k)\right]^T \tag{19}$$

$$\Psi'(\nu_k) = \begin{bmatrix} \psi'(\nu^1_k) & \cdots & 0 \\ \vdots & \ddots & \vdots \\ 0 & \cdots & \psi'(\nu^m_k) \end{bmatrix}^T \tag{20}$$

The nonlinear function $\psi(\cdot)$ for the class of ε contaminated distributions of probabilities is Huber's function [42], and it is obtained with the application of game theory in statistics. It is defined on the basis of the least favorable distribution of probability for the given class of probability distribution. The nonlinear function $\psi(\cdot)$ can be chosen as

$$\psi(t) = \begin{cases} t, & |t| \le L \\ L\cdot\mathrm{sgn}(t), & |t| > L \end{cases} \tag{21}$$

where L is a constant depending on ε.

3.2. Prediction with adaptation of the process noise covariance

The predicted state estimate can be derived by using the unscented transform technique

$$\hat{x}_{k|k-1} = \sum_{s=0}^{2n}\omega_s f(\chi^s_{k-1}) \tag{22}$$

$$P^*_{k|k-1} = \sum_{s=0}^{2n}\omega_s[f(\chi^s_{k-1}) - \hat{x}_{k|k-1}][f(\chi^s_{k-1}) - \hat{x}_{k|k-1}]^T \tag{23}$$

$$P_{k|k-1} = P^*_{k|k-1} + \hat{Q}_{k-1} \tag{24}$$

where the weights ω_s and the sigma points χ^s_{k-1} are given by

$$\chi^0_{k-1} = \hat{x}_{k-1|k-1},\ \omega_0 = \frac{\kappa}{n+\kappa} \tag{25}$$

$$\chi^s_{k-1} = \hat{x}_{k-1|k-1} + (\sqrt{(n+\kappa)P_{k-1|k-1}})_s,$$

$$\omega_s = \frac{1}{2(n+\kappa)},\ s = 1, \cdots, n \tag{26}$$

$$\chi^{s+n}_{k-1} = \hat{x}_{k-1|k-1} - (\sqrt{(n+\kappa)P_{k-1|k-1}})_s,$$

$$\omega_s = \frac{1}{2(n+\kappa)},\ s = 1, \cdots, n \tag{27}$$

Note that the process noise covariance $\hat{Q}_{k-1}$ is used to derive the covariance $P_{k|k-1}$ in (24). Since the process noise covariance matrix is usually unknown (e.g., tracking a maneuvering vehicle [40]), the covariance matrix should be adjusted recursively. To derive the estimated covariance $\hat{Q}_{k-1}$, an adaptive factor is used to adjust the covariance as follows [43]

$$\hat{Q}_{k-1} = \lambda_{k-1}\bar{Q}_{k-1} \tag{28}$$

where $\bar{Q}_{k-1}$ is the pre-designed covariance and λ_k is the adaptive factor calculated by

$$\lambda_{k-1} = \frac{a_{k-1}}{b_{k-1}} \tag{29}$$

where

$$a_{k-1} = \mathrm{Tr}\{\hat{R}_k\} + \mathrm{Tr}\{[P^{xz}_{k|k-1}]^T\bar{P}^{-1}_{k|k-1}K_k\Psi'(\nu_k)K^T_kP^{xz}_{k|k-1}\bar{P}^{-1}_{k|k-1}\} - \eta^T_k\eta_k - \mathrm{Tr}\{[P^{xz}_{k|k-1}]^T\bar{P}^{-1}_{k|k-1}P^*_{k|k-1}P^{xz}_{k|k-1}\bar{P}^{-1}_{k|k-1}\} \tag{30}$$

$$b_{k-1} = \mathrm{Tr}\{[P^{xz}_{k|k-1}]^T\bar{P}^{-1}_{k|k-1}\bar{Q}_{k-1}P^{xz}_{k|k-1}\bar{P}^{-1}_{k|k-1}\} \tag{31}$$

See Appendix A for the derivations of a_{k-1} and b_{k-1}.

For clarity, the proposed filter is formulated as Algorithm 3.

Remark 1. In this paper, the process noise is assumed to be Gaussian with unknown covariance matrix, and the measurement noise is assumed to be a mixture of two Gaussian components with unknown covariance matrices. The aim of the proposed filter is to jointly estimate the state estimate and the covariance matrices, where two different adaptation strategies are adopted to estimate the noise covariance matrices Q_{k-1} and R_k, respectively. To be specific, the estimated process noise covariance $\hat{Q}_{k-1}$ is adjusted based on a pre-designed covariance $\bar{Q}_{k-1}$, while the estimated measurement noise covariance $\hat{R}_k$ is derived by applying the moving window approach to the innovations. It should be pointed out that the proposed adaptation strategies can be combined with the Kalman filter and the EKF to improve the robustness against the noise uncertainty.

Remark 2. In contrast to the Masreliez–Martin EKF in [18], the UKF is adopted to address the nonlinear Bayesian problem in this paper. Moreover, the noise covariance matrices have been estimated recursively, while they are assumed to be known in [18]. Compared with the robust adaptive UKF in [38], the Masreliez–Martin method is adopted to derive the updated state estimate in the proposed filter. Moreover, the measurement noise covariance R_k is estimated directly in this paper while an adaptive factor is adopted to adjust the measurement noise covariance in [38]. This is because the noise covariance matrices are assumed to be known in the robust adaptive UKF [38] and the aim of adaptation is to make the filter robust against faults in both system and measurements.

4. Monte Carlo simulation results

In this section, two numerical examples are provided to illustrate the effectiveness of the proposed filter.

Example 1. To compare the performance of the proposed filter with that of the PMCMC method, we consider the following example [24]

$$x_k = \frac{1}{2}x_{k-1} + \frac{25x_{k-1}}{1+x_{k-1}^2} + 8\cos(1.2k) + w_{k-1} \tag{32}$$

$$z_k = \frac{1}{20}x_k^2 + v_k \tag{33}$$

where the variance parameters are set $Q_k = 1$, $R_{k,1} = 1$, and $R_{k,2} = 10$. The contamination probability is taken $\varepsilon = 0.1$. The PMCMC algorithm is implemented by using 500 particles and the number of iterations in the MCMC samplers is 3000. The estimation errors are shown in Fig. 1, which suggest that the PMCMC algorithm outperforms the proposed filter. However, it is worth mentioning here that the PMCMC algorithm consumes a higher computational cost than the proposed filter since a large number of particles have been used.

Example 2. A simulated relative navigation scenario is used to evaluate the performance of the proposed filter when the measurement noise is contaminated with glint noise. Several other robust UKF algorithms were also evaluated to demonstrate the improved performance of the proposed filter.

Two spacecrafts are designated as the chief spacecraft and the deputy spacecraft, respectively. The Hill coordinate frame is used in this paper, which is a Cartesian, rectangular, dextral rotating frame centered on the chief and also referred to as the local-vertical-local-horizontal (LVLH) frame. The equation of motion for

Algorithm 3: The proposed Masreliez–Martin UKF.

Given the state estimates $\hat{x}_{1|0}$ and its associated error covariance $P_{1|0}$ at time $k = 0$. Compute the state estimate at every time k as follows.

Step 1. Update

Step 1.1. Generate the sigma points

$$\chi_{k|k-1}^0 = \hat{x}_{k|k-1},\ \omega_0 = \frac{\kappa}{n+\kappa}$$
$$\chi_{k|k-1}^s = \hat{x}_{k|k-1} + (\sqrt{(n+\kappa)P_{k|k-1}})_s,\ \omega_s = \frac{1}{2(n+\kappa)},\ s = 1,\cdots,n$$
$$\chi_{k|k-1}^{s+n} = \hat{x}_{k|k-1} - (\sqrt{(n+\kappa)P_{k|k-1}})_s,\ \omega_s = \frac{1}{2(n+\kappa)},\ s = 1,\cdots,n$$

Step 1.2. Calculate the estimate of the measurement noise covariance

$$\hat{z}_{k|k-1} = \sum_{s=0}^{2n} \omega_s h(\chi_{k|k-1}^s)$$
$$P_{k|k-1}^{xz} = \sum_{s=0}^{2n} \omega_s [\chi_{k|k-1}^s - \hat{x}_{k|k-1}][\chi_{k|k-1}^s - \hat{x}_{k|k-1}]^T$$
$$P_{k|k-1}^{zz} = \sum_{s=0}^{2n} \omega_s [h(\chi_{k|k-1}^s) - \hat{z}_{k|k-1}][h(\chi_{k|k-1}^s) - \hat{z}_{k|k-1}]$$
$$e_{k-j} = z_k - \hat{z}_{k-j|k-j-1}$$
$$\hat{R}_k^* = \frac{1}{N}\sum_{j=0}^{N-1} e_{k-j}e_{k-j}^T - P_{k|k-1}^{zz}$$
$$\hat{R}_k = \mathrm{diag}\{|\hat{R}_k^*(1)|, |\hat{R}_k^*(2)|, \cdots, |\hat{R}_k^*(m)|\}$$
$$P_{k|k-1}^{ee} = P_{k|k-1}^{zz} + \hat{R}_k$$

Step 1.3. Calculate the updated estimates

$$\hat{x}_{k|k} = \hat{x}_{k|k-1} + K_k\Psi(\nu_k)$$
$$P_{k|k} = P_{k|k-1} - K_k\Psi'(\nu_k)K_k^T$$
$$\nu_k = [P_{k|k-1}^{ee}]^{-1/2}e_k$$
$$K_k = P_{k|k-1}^{xz}[P_{k|k-1}^{ee}]^{-T/2}$$
$$\Psi(\nu_k) = \left[\psi(\nu_k^1) \quad \cdots \quad \psi(\nu_k^m)\right]^T$$
$$\Psi'(\nu_k) = \begin{bmatrix} \psi'(\nu_k^1) & \cdots & 0 \\ \vdots & \ddots & \vdots \\ 0 & \cdots & \psi'(\nu_k^m) \end{bmatrix}$$
$$\psi(t) = \begin{cases} t, & |t| \le L \\ L\cdot\mathrm{sgn}(t), & |t| > L \end{cases}$$

Step 2. Prediction

Step 2.1. Generate sigma points

$$\chi_{k-1}^0 = \hat{x}_{k-1|k-1},\ \omega_0 = \frac{\kappa}{n+\kappa}$$
$$\chi_{k-1}^s = \hat{x}_{k-1|k-1} + (\sqrt{(n+\kappa)P_{k-1|k-1}})_s,\ \omega_s = \frac{1}{2(n+\kappa)},\ s = 1,\cdots,n$$
$$\chi_{k-1}^{s+n} = \hat{x}_{k-1|k-1} - (\sqrt{(n+\kappa)P_{k-1|k-1}})_s,\ \omega_s = \frac{1}{2(n+\kappa)},\ s = 1,\cdots,n$$

Step 2.2. Calculate the estimate of the process noise covariance

$$\hat{Q}_{k-1} = \lambda_{k-1}\bar{Q}_{k-1}$$
$$\lambda_{k-1} = \frac{a_{k-1}}{b_{k-1}}$$
$$a_{k-1} = \mathrm{Tr}\{\hat{R}_k\} + \mathrm{Tr}\{[P_{k|k-1}^{xz}]^T\bar{P}_{k|k-1}^{-1}K_k\Psi'(\nu_k)K_k^TP_{k|k-1}^{xz}\bar{P}_{k|k-1}^{-1}\}$$
$$\quad - \eta_k^T\eta_k - \mathrm{Tr}\{[P_{k|k-1}^{xz}]^T\bar{P}_{k|k-1}^{-1}P_{k|k-1}^*P_{k|k-1}^{xz}\bar{P}_{k|k-1}^{-1}\}$$
$$b_{k-1} = \mathrm{Tr}\{[P_{k|k-1}^{xz}]^T\bar{P}_{k|k-1}^{-1}\bar{Q}_{k-1}P_{k|k-1}^{xz}\bar{P}_{k|k-1}^{-1}\}$$

Step 2.3. Calculate the predicted estimates

$$\hat{x}_{k|k-1} = \sum_{s=0}^{2n}\omega_s f(\chi_{k-1}^s)$$
$$P_{k|k-1}^* = \sum_{s=0}^{2n}\omega_s[f(\chi_{k-1}^s) - \hat{x}_{k|k-1}][f(\chi_{k-1}^s) - \hat{x}_{k|k-1}]^T$$
$$P_{k|k-1} = P_{k|k-1}^* + \hat{Q}_{k-1}$$

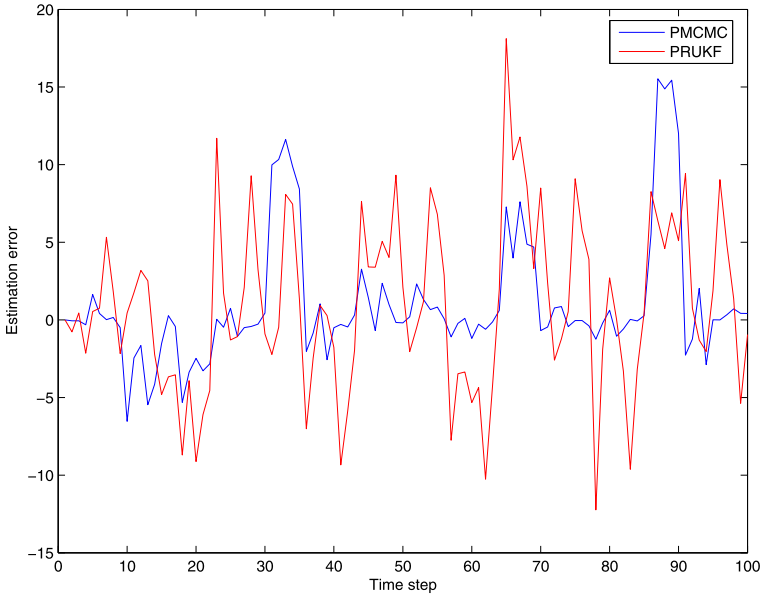

Fig. 1. Estimation error via time step.

the deputy spacecraft relative to the chief spacecraft in the Hill frame can be expressed as [44]

$$\ddot{x} = 2\omega\dot{y} + \dot{\omega}y + \omega^2 x + \frac{\mu}{r_c^2} - \frac{\mu(r_c + x)}{[(r_c + x)^2 + y^2 + z^2]^{3/2}} + w_x \tag{34}$$

$$\ddot{y} = -2\omega\dot{x} - \dot{\omega}x + \omega^2 y - \frac{\mu y}{[(r_c + x)^2 + y^2 + z^2]^{3/2}} + w_y \tag{35}$$

$$\ddot{z} = -\frac{\mu(r_c + x)}{[(r_c + x)^2 + y^2 + z^2]^{3/2}} + w_z \tag{36}$$

with

$$\ddot{r}_c = r_c\omega^2 - \frac{\mu}{r_c^2} \tag{37}$$

$$\dot{\omega} = -\frac{2\dot{r}_c\omega}{r_c} \tag{38}$$

where x, y, and z are the radial, in-track and cross-track coordinates of the Hill frame, respectively. r_c is the distance of the chief spacecraft in the inertial coordinate frame. μ is the gravitational parameter of the central body. ω is the orbital angular velocity of the chief spacecraft. w_x, w_y, and w_z are modeled as zero-mean white Gaussian noise with variances of σ_x^2, σ_y^2 and σ_z^2, respectively.

The radar system located on the chief spacecraft provides the measurements including the relative range between the chief and the deputy, the azimuth angle, and the elevation angle

$$\rho = \sqrt{x^2 + y^2 + z^2} + v_\rho \tag{39}$$

$$\theta = \arctan\frac{y}{x} + v_\theta \tag{40}$$

$$\phi = \arctan\frac{z}{\sqrt{x^2 + y^2}} + v_\phi \tag{41}$$

where ρ denotes the relative range, θ denotes the azimuth angle and ϕ denotes the elevation angle. The measurement noise $v_k = [v_\rho\ v_\theta\ v_\phi]^T$ is assumed to be contaminated by the glint noise and is represented by [45,46]

$$p(v_k) = (1 - \varepsilon)\mathcal{N}(v_k, 0, R_{k,1}) + \varepsilon\mathcal{N}(v_k, 0, R_{k,2}) \tag{42}$$

The relative trajectory of the chief and the deputy spacecrafts are propagated by using the fixed-step 4th-order Runge–Kutta algorithm. The state vector $\mathbf{x}_k = [x_k\ y_k\ z_k\ \dot{x}_k\ \dot{y}_k\ \dot{z}_k]^T$ consists of the relative position and velocity components.

The true initial state for this relative navigation is taken to be

$x_0 = 31.9262$ km,

$y_0 = -7.1384$ km,

$z_0 = 33.4729$ km

$\dot{x}_0 = -0.005583$ km/s,

$\dot{y}_0 = -0.071774$ km/s,

$\dot{z}_0 = 0.026249$ km/s

The initial estimates are assumed to be with small errors

$\hat{x}_0 = 31.9262$ km,

$\hat{y}_0 = -8.1384$ km,

$\hat{z}_0 = 32.4729$ km

$\hat{\dot{x}}_0 = -0.004416$ km/s,

$\hat{\dot{y}}_0 = -0.061774$ km/s,

$\hat{\dot{z}}_0 = 0.036249$ km/s

and the initial covariance matrix is set as

$$P_0 = \mathrm{diag}\{[1^2, 1^2, 1^2](\mathrm{km})^2, [0.01^2, 0.01^2, 0.01^2](\mathrm{km/s})^2\}$$

The simulation time is 20 min. The prediction of the filter is performed every 0.01 s and the period state update interval with radar measurement is set to be 1 s. The deputy spacecraft's eccentricity and semimajor axis are set as $e_c = 0.146$ and $a_c = 8000$ km, respectively. The standard deviations of process noise w_x, w_y, w_z are assumed to be 10^{-4} km/s^2. The measurement noise covariance matrices are taken to be $R_{k,1} = \mathrm{diag}\{10^2, (0.05\pi/180)^2, (0.05\pi/180)^2\}$ and $R_{k,2} = \mathrm{diag}\{60^2, (0.5\pi/180)^2, (0.5\pi/180)^2\}$, respectively. The contaminating parameter is taken to be $\varepsilon = 0.1$. To estimate the measurement noise covariance matrix in the proposed filter, the window width is set as $N = 15$.

The performance of the proposed robust UKF (PRUKF) was compared against the UKF [29], the unscented H_∞ filter (UHF) [30],

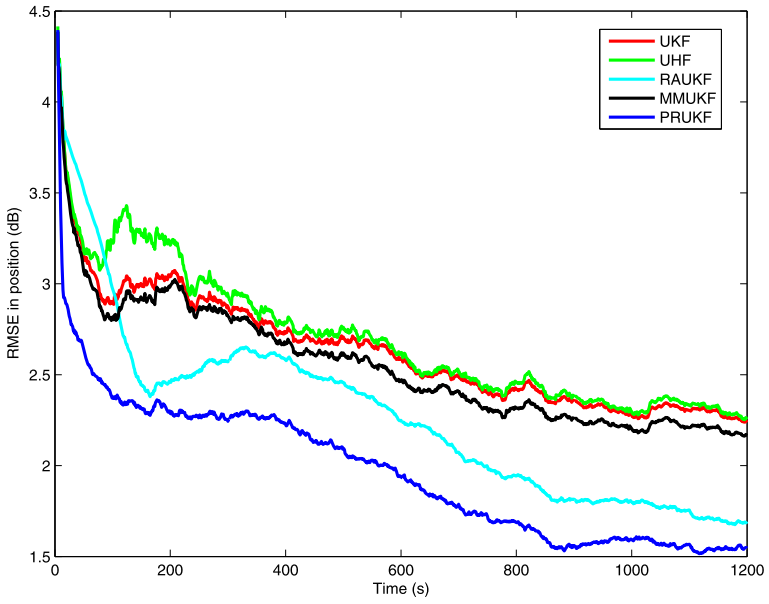

Fig. 2. Performance comparison with respect to RMSE in position.

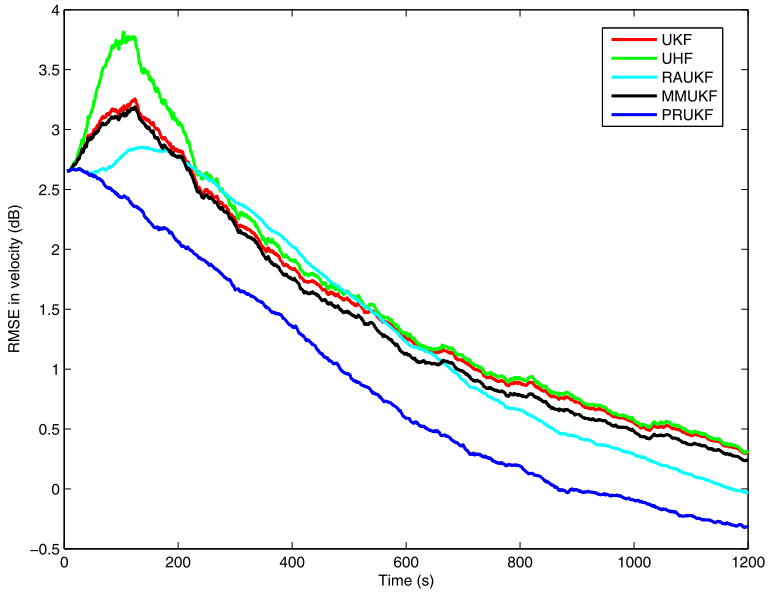

Fig. 3. Performance comparison with respect to RMSE in velocity.

the modified Masreliez–Martin UKF (MMUKF) [18] (Note that the EKF is used in the Masreliez–Martin filter, the UKF is adopted in this paper for a fair comparison) and the robust adaptive UKF (RAUKF) [38]. To illustrate the performance of the filters, the root mean square error (RMSE) in position and velocity are shown and the simulation results are derived from 100 Monte Carlo runs. The RMSE in position and velocity are shown in Fig. 2 and Fig. 3, respectively. The simulation results suggest that the performance of the UKF can be improved by applying adaptation strategies to the process and measurement noise covariances. It should be pointed out that the UHF might not always performs better than the UKF since the performance level is difficult to be adjusted to improve the performance [30]. In addition, it can be observed that the proposed filter outperforms the MMUKF and the RAUKF. This is due to the fact that the advantages of the MMUKF and the RAUKF have been inherited in the proposed filter.

To illustrate the performance of the proposed filter with different levels of measurement noise covariance, the averaged RMSE with different contaminating parameters are displayed in Fig. 4 and Fig. 5. From the simulations, it appears that the performance of the filters is degraded as the contaminating parameter ε increases. This is reasonable since the noise covariance $R_{k,2}$ is larger than $R_{k,1}$. Note that the proposed filter always performs the best among the filters.

5. Robot arm tracking experimental results

This section presents experimental results demonstrating the performance of the proposed filter applied to vision-aided robot arm tracking system. The Kalman filter has been used to track the robot arm using low cost 3D vision systems in [47]. In this paper, we show that the performance can be improved greatly by using robust UKF with adaptation of noise covariances.

As shown in Fig. 6, the experiment system is a ABB IRB 120-3/0.6 robot arm. The vision system used in this experiment consists of two optical sensors. Both sensors are RGB cameras

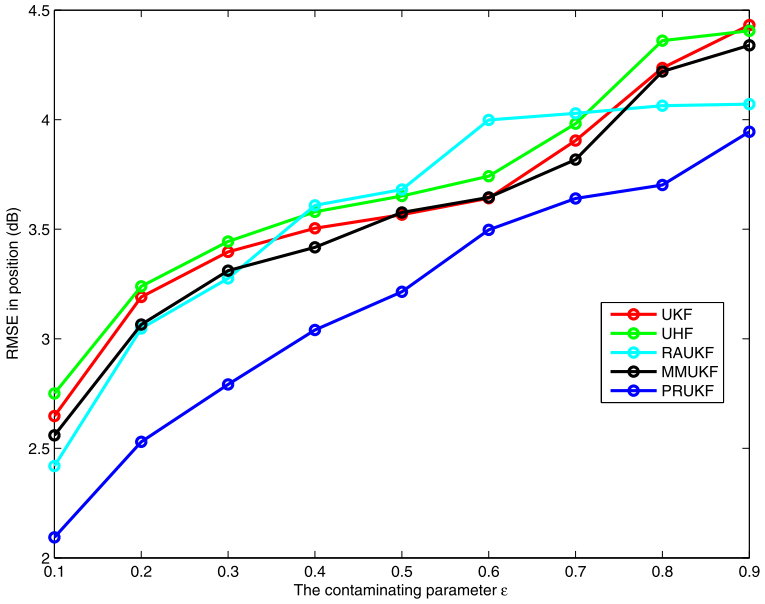

Fig. 4. Averaged RMSE in position with respect to the contaminating parameter.

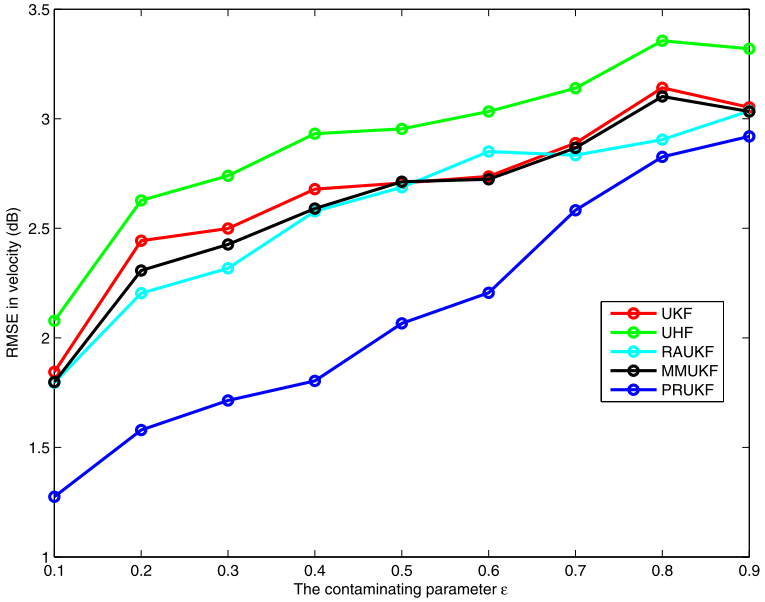

Fig. 5. Averaged RMSE in velocity with respect to the contaminating parameter.

which have a video resolution of 30 fps. The image resolution given by this camera is 640 × 480 pixels. The calibration of the cameras is needed to relate both cameras and robot coordinates reference systems so that the objects located by the camera can be handled by the robot. The intrinsic parameters of the vision system are calibrated by the standard procedure as shown in [48].

We consider a three-dimensional dynamic model for the robot arm motion. The state of the robot arm is denoted by $x = [\xi\ \ \theta\ \ \psi\ \ q_1\ \ q_2\ \ q_3\ \ q_4\ \ q_5\ \ q_6]^T$, where $p = (\xi\ \ \theta\ \ \psi)$, and $q = (q_1\ \ q_2\ \ q_3\ \ q_4\ \ q_5\ \ q_6)$ represent the position vector and the joint angle vector, respectively. The robot arm kinematic equation can be represented by [49]

$$\dot{p} = J(q)\dot{q} \tag{43}$$

$$\dot{q} = w \tag{44}$$

where w is the process noise with zero-mean white Gaussian and

$$J(q) = \begin{bmatrix} J_{11} & J_{12} & J_{13} & J_{14} & J_{15} & 0 \\ J_{21} & J_{22} & J_{23} & J_{24} & J_{25} & 0 \\ 0 & J_{32} & J_{33} & J_{34} & J_{35} & 0 \end{bmatrix} \tag{45}$$

The elements of the matrix J are given by

$$J_{11} = d_2 s_{23} s_1 - s_1(a_2 c_{23} + a_1 c_2) - d_3(s_5(c_1 s_4 - c_{23} c_4 s_1) - s_{23} c_5 s_1) \tag{46}$$

$$J_{21} = c_1(a_2 c_{23} + a_1 c_2) - d_3(s_5(s_1 s_4 + c_{23} c_1 c_4) + s_{23} c_1 c_5) - d_2 s_{23} c_1 \tag{47}$$

$$J_{12} = -d_3(c_{23} c_1 c_5 - s_{23} c_1 c_4 c_5) - c_1(a_2 s_{23} + a_1 s_2) - d_2 c_{23} c_1 \tag{48}$$

$$J_{22} = -d_3(c_{23} c_5 s_1 - s_{23} c_4 s_1 s_5) - s_1(a_2 s_{23} + a_1 s_2) - d_2 c_{23} s_1 \tag{49}$$

$$J_{32} = d_4 s_{23} - a_2 c_{23} - a_1 c_2 + d_3(s_{23} c_5 + c_{23} c_4 s_5) \tag{50}$$

Fig. 6. The ABB IRB 120-3/0.6 robot arm tracking system.

$$J_{13} = -d_3(c_{23}c_1c_5 - s_{23}c_1c_4c_5) - d_4c_{23}c_1 - a_2s_{23}c_1 \tag{51}$$

$$J_{23} = -d_3(c_{23}c_5s_1 - s_{23}c_4s_1s_5) - d_4c_{23}s_1 - a_2s_{23}s_1 \tag{52}$$

$$J_{33} = d_2s_{23} - a_2c_{23} + d_3(s_{23}c_5 + c_{23}c_4s_5) \tag{53}$$

$$J_{14} = -d_3s_5(c_4s_1 - c_{23}c_1s_4) \tag{54}$$

$$J_{24} = d_3s_5(c_1c_4 + c_{23}s_1s_4) \tag{55}$$

$$J_{34} = -d_3s_{23}s_4s_5 \tag{56}$$

$$J_{15} = -d_3(c_5(s_1s_4 + c_{23}c_1c_4) - s_{23}c_1c_5) \tag{57}$$

$$J_{25} = d_3(c_5(c_1s_4 - c_{23}c_4s_1) + s_{23}s_1s_5) \tag{58}$$

$$J_{35} = d_3(c_{23}s_5 + s_{23}c_4c_5) \tag{59}$$

where $a_1 = 270$ mm, $a_2 = 70$ mm, $d_1 = 290$ mm, $d_2 = 302$ mm, $d_3 = 179$ mm are parameters of the robot arm, and

$$c_i = \cos(q_i), \quad c_{ij} = \cos(q_i + q_j) \tag{60}$$

$$s_i = \sin(q_i), \quad s_{ij} = \sin(q_i + q_j), \quad i, j = 1, \cdots, 5. \tag{61}$$

The measurement data from both cameras and the odometry are used to improve the tracking performance. By using the coordinate transformation from the camera frame to the robot frame, the measurement equation can be represented by

$$z_k = x_k + v_k \tag{62}$$

where v_k is the measurement noise with zero mean white Gaussian.

Similar to the comparisons in the relative navigation simulations, the performance of the proposed PRUKF is compared with the UKF, the UHF, the MMUKF and the RAUKF. To implement the filters, the standard deviation of the process noise is taken to be 0.1. The standard deviation of the measurement noise covariance matrix is taken to be 10 for position in each axis and 0.01 for joint angles. To estimate the measurement noise covariance matrix in the proposed filter, the window width is set as $N = 15$. The sampling time interval is 0.1 s and the simulation time is 60 s.

The trajectory of the robot arm is shown in Fig. 7, where the actual position are derived by using the CPos of the robot arm software. The estimation errors are shown in Fig. 8, in which the simulation results show that the performance of the UKF, the UHF and the MMUKF are almost identical since the noise covariance matrices are not adjusted in these filters. In addition, it can be observed that the proposed PRUKF performs better than the other filters.

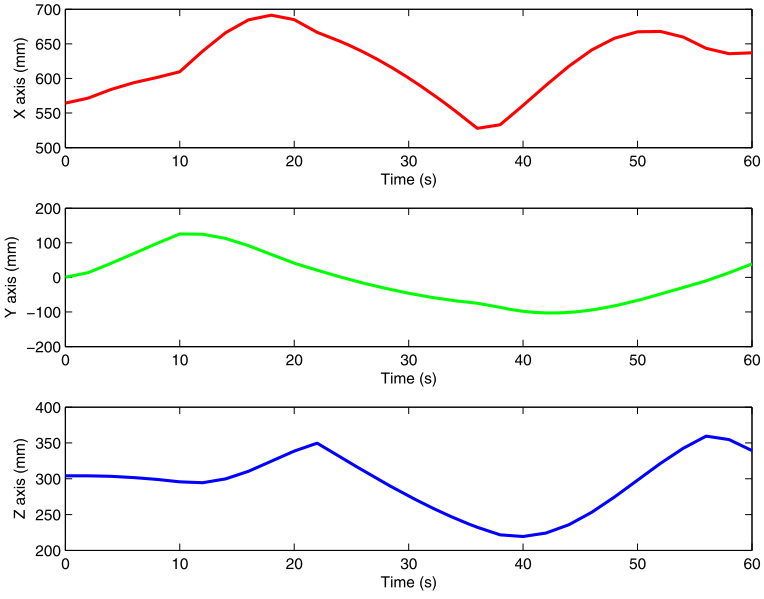

Fig. 7. Trajectory of the robot arm.

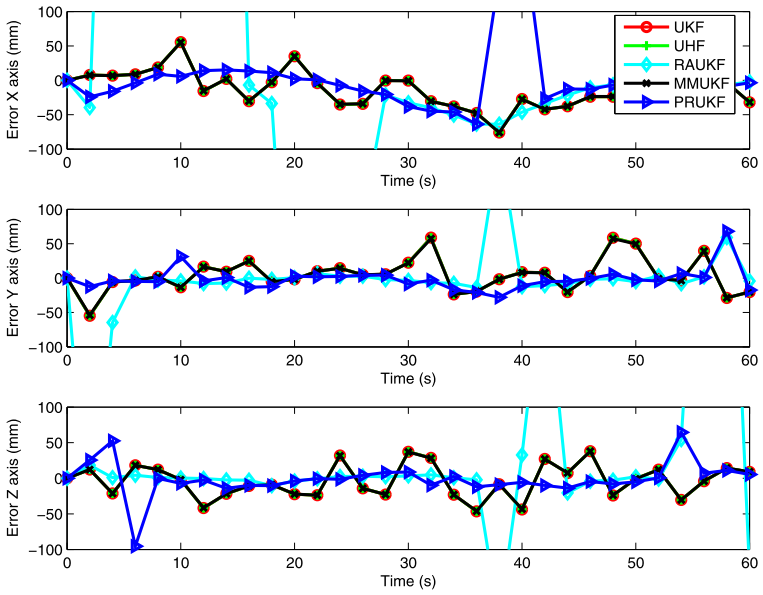

Fig. 8. Estimation error versus time.

6. Conclusion

In this paper, a modified Masreliez–Martin UKF is developed for discrete-time nonlinear stochastic systems. The process noise and the measurement noise covariance matrices are adaptively adjusted at each time step. The proposed filter is derivative-free and is easy to be implemented. Simulation and experiment results show that the proposed filter outperforms the existing robust filters. Future work will focus on uniformly asymptotical stability analysis for the proposed filter as in [9,19,21].

Acknowledgments

The authors would like to thank Dr. Fredrik Lindsten for providing the PMCMC code on the website (http://users.isy.liu.se/en/rt/lindsten/code.html). This work was supported by the National Basic Research Program of China (973 Program, 2012CB821200, 2012CB821201), the NSFC (61573031, 61134005, 61203044, 61221061, 61327807, 61320106006, 61473010, 61473015) and the Beijing Natural Science Foundation (4132040).

Appendix A

As shown in [38], the covariance of the residual η_k can be represented by

$$P_\eta = \hat{R}_k - [P^{xz}_{k|k-1}]^T \bar{P}^{-1}_{k|k-1} P_{k|k} P^{xz}_{k|k-1} \bar{P}^{-1}_{k|k-1} \tag{A.1}$$

where

$$\bar{P}_{k|k-1} = P^*_{k|k-1} + \bar{Q}_{k-1} \tag{A.2}$$

Substituting (16) into (A.1) leads to

$$\begin{aligned} P_\eta &= \hat{R}_k - [P^{xz}_{k|k-1}]^T \bar{P}^{-1}_{k|k-1} (P_{k|k-1} - K_k \Psi'(\nu_k) K_k^T) P^{xz}_{k|k-1} \bar{P}^{-1}_{k|k-1} \\ &= \hat{R}_k - [P^{xz}_{k|k-1}]^T \bar{P}^{-1}_{k|k-1} (P^*_{k|k-1} + \hat{Q}_{k-1}) P^{xz}_{k|k-1} \bar{P}^{-1}_{k|k-1} \\ &\quad + [P^{xz}_{k|k-1}]^T \bar{P}^{-1}_{k|k-1} K_k \Psi'(\nu_k) K_k^T P^{xz}_{k|k-1} \bar{P}^{-1}_{k|k-1} \end{aligned} \tag{A.3}$$

Taking trace operator on both sides of (A.3) yields

$$\begin{aligned} \mathrm{Tr}\{P_\eta\} &= \mathrm{Tr}\{\hat{R}_k\} - \mathrm{Tr}\{[P^{xz}_{k|k-1}]^T \bar{P}^{-1}_{k|k-1} P^*_{k|k-1} P^{xz}_{k|k-1} \bar{P}^{-1}_{k|k-1}\} \\ &\quad - \lambda_{k-1} \mathrm{Tr}\{[P^{xz}_{k|k-1}]^T \bar{P}^{-1}_{k|k-1} \bar{Q}_{k-1} P^{xz}_{k|k-1} \bar{P}^{-1}_{k|k-1}\} \\ &\quad + \mathrm{Tr}\{[P^{xz}_{k|k-1}]^T \bar{P}^{-1}_{k|k-1} K_k \Psi'(\nu_k) K_k^T P^{xz}_{k|k-1} \bar{P}^{-1}_{k|k-1}\} \end{aligned} \tag{A.4}$$

On the other hand, it is assumed that the covariance of the residual can be approximated by

$$\begin{aligned} P_\eta &= \mathrm{E}\{\eta_k \eta_k^T\} \\ &= \eta_k \eta_k^T \end{aligned} \tag{A.5}$$

Substituting (A.5) into (A.4) we can get

$$\begin{aligned} \eta_k^T \eta_k &= \mathrm{Tr}\{\hat{R}_k\} - \mathrm{Tr}\{[P^{xz}_{k|k-1}]^T \bar{P}^{-1}_{k|k-1} P^*_{k|k-1} P^{xz}_{k|k-1} \bar{P}^{-1}_{k|k-1}\} \\ &\quad - \lambda_{k-1} \mathrm{Tr}\{[P^{xz}_{k|k-1}]^T \bar{P}^{-1}_{k|k-1} \bar{Q}_{k-1} P^{xz}_{k|k-1} \bar{P}^{-1}_{k|k-1}\} \\ &\quad + \mathrm{Tr}\{[P^{xz}_{k|k-1}]^T \bar{P}^{-1}_{k|k-1} K_k \Psi'(\nu_k) K_k^T P^{xz}_{k|k-1} \bar{P}^{-1}_{k|k-1}\} \end{aligned} \tag{A.6}$$

Then we can get the adaptive scaling factor

$$\lambda_{k-1} = \frac{a_{k-1}}{b_{k-1}} \tag{A.7}$$

where

$$\begin{aligned} a_{k-1} &= \mathrm{Tr}\{\hat{R}_k\} + \mathrm{Tr}\{[P^{xz}_{k|k-1}]^T \bar{P}^{-1}_{k|k-1} K_k \Psi'(\nu_k) K_k^T P^{xz}_{k|k-1} \bar{P}^{-1}_{k|k-1}\} \\ &\quad - \eta_k^T \eta_k - \mathrm{Tr}\{[P^{xz}_{k|k-1}]^T \bar{P}^{-1}_{k|k-1} P^*_{k|k-1} P^{xz}_{k|k-1} \bar{P}^{-1}_{k|k-1}\} \end{aligned} \tag{A.8}$$

$$b_{k-1} = \mathrm{Tr}\{[P^{xz}_{k|k-1}]^T \bar{P}^{-1}_{k|k-1} \bar{Q}_{k-1} P^{xz}_{k|k-1} \bar{P}^{-1}_{k|k-1}\} \tag{A.9}$$

References

[1] F. Auger, M. Hilairet, J.M. Guerrero, E. Monmasson, T. Orlowska-Kowalska, S. Katsura, Industrial applications of the Kalman filter: a review, IEEE Trans. Ind. Electron. 60 (12) (2013) 5458–5471.

[2] D. Simon, Optimal State Estimation: Kalman, H_∞ and Nonlinear Approaches, Wiley, New York, 2006.

[3] C.J. Masreliez, R.D. Martin, Robust Bayesian estimation for the linear model and robustifying the Kalman filter, IEEE Trans. Autom. Control 22 (3) (1977) 361–371.

[4] M.C. Graham, J.P. How, D.E. Gustafson, Robust state estimation with sparse outliers, J. Guid. Control Dyn. 38 (7) (2015) 1229–1240, http://dx.doi.org/10.2514/1.G000350.

[5] I.C. Schick, S.K. Mitter, Robust recursive estimation in the presence of heavy-tailed observation noise, Ann. Stat. 22 (2) (1994) 1045–1080.

[6] G. Agamennoni, J.I. Nieto, E.M. Nebot, Approximate inference in state-space models with heavy-tailed noise, IEEE Trans. Signal Process. 60 (10) (2012) 5024–5037.

[7] G. Chang, M. Liu, M-estimator-based robust Kalman filter for systems with process modeling errors and rank deficient measurement models, Nonlinear Dyn. 80 (2015) 1431–1449.
[8] K.H. Kim, J.G. Lee, C.G. Park, Adaptive two-stage Kalman filter in the presence of unknown random bias, Int. J. Adapt. Control Signal Process. 20 (7) (2006) 305–319.
[9] K.H. Kim, J.G. Lee, C.G. Park, The stability analysis of the adaptive two-stage Kalman filter, Int. J. Adapt. Control Signal Process. 21 (10) (2007) 856–870.
[10] Y.X. Yang, T.H. Xu, An adaptive Kalman filter based on sage windowing weights and variance components, J. Navig. 56 (2) (2003) 231–240.
[11] Y.X. Yang, W.G. Gao, An optimal adaptive Kalman filter, J. Geod. 80 (4) (2006) 178–183.
[12] Y. Yang, S. Zhang, Adaptive fitting of systematic errors in navigation, J. Geod. 79 (1–3) (2005) 43–49.
[13] W. Shen, L. Deng, Game theory approach to discrete H_∞ filter design, IEEE Trans. Signal Process. 45 (4) (1997) 1092–1095.
[14] S. Sarkka, A. Nummenmaa, Recursive noise adaptive Kalman filtering by variational Bayesian approximations, IEEE Trans. Autom. Control 54 (3) (2009) 596–600.
[15] A.H. Mohamed, K.P. Schwarz, Adaptive Kalman filtering for INS/GPS, J. Geod. 73 (4) (1999) 193–203.
[16] W. Li, D. Gong, M. Liu, J. Chen, D. Duan, Adaptive robust Kalman filter for relative navigation using global position system, IET Radar Sonar Navig. 7 (5) (2013) 471–479.
[17] G. Chang, Kalman filter with both adaptivity and robustness, J. Process Control 24 (3) (2014) 81–87.
[18] V. Stojanovic, N. Nedic, Robust Kalman filtering for nonlinear multivariable stochastic systems in the presence of non-Gaussian noise, Int. J. Robust Nonlinear Control (2015), http://dx.doi.org/10.1002/rnc.3319.
[19] K.H. Kim, G.I. Lee, C.G. Park, J.G. Lee, The stability analysis of the adaptive fading extended Kalman filter using the innovation covariance, Int. J. Control. Autom. Syst. 7 (1) (2009) 49–56.
[20] Y. Xing, S. Zhang, J. Zhang, X. Cao, Robust-extended Kalman filter for small satellite attitude estimation in the presence of measurement uncertainties and faults, Proceedings of the Institution of Mechanical Engineers, Part G, J. Aerosp. Eng. 226 (1) (2012) 30–41.
[21] C. Bicer, E.K. Babacan, L. Ozbek, Stability of the adaptive fading extended Kalman filter with the matrix forgetting factor, Turk. J. Electr. Eng. Comput. Sci. 20 (5) (2012) 819–833.
[22] C.D. Karlgaard, H. Schaub, Huber-based divided difference filtering, J. Guid. Control Dyn. 30 (3) (2007) 885–891.
[23] C.D. Karlgaard, H. Schaub, Adaptive nonlinear Huber-based navigation for rendezvous in elliptical orbit, J. Guid. Control Dyn. 34 (2) (2011) 388–402.
[24] C. Andrieu, A. Doucet, R. Holenstein, Particle Markov chain Monte Carlo methods, J. R. Stat. Soc. B 72 (3) (2010) 269–342.
[25] C.M. Carvalho, M.S. Johannes, H.F. Lopes, N.G. Polson, Particle learning and smoothing, Stat. Sci. 25 (1) (2010) 88–106.
[26] N. Chopin, P.E. Jacob, O. Papaspiliopoulos, SMC2: an efficient algorithm for sequential analysis of state space models, J. R. Stat. Soc. B 75 (3) (2013) 397–426.
[27] D. Crisan, J. Miguez, Nested particle filters for online parameter estimation in discrete-time state-space Markov models, arXiv:1308.1883, 2013.
[28] L. Martino, F. Leisen, J. Corander, On multiple try schemes and the particle Metropolis–Hastings algorithm, arXiv:1409.0051, 2014.
[29] S.J. Julier, J.K. Uhlmann, H.F. Durrant-Whyte, A new method for the nonlinear transformation of means and covariances in filters and estimator, IEEE Trans. Autom. Control 45 (3) (2010) 477–482.
[30] W.L. Li, Y.M. Jia, H-infinity filtering for a class of nonlinear discrete-time systems based on unscented transform, Signal Process. 90 (12) (2010) 3301–3307.
[31] H.E. Soken, C. Hajiyev, Pico satellite attitude estimation via robust unscented Kalman filter in the presence of measurement faults, ISA Trans. 49 (3) (2010) 249–256.
[32] C. Hajiyev, Fault tolerant integrated radar/inertial altimeter based on nonlinear robust adaptive Kalman filter, Aerosp. Sci. Technol. 17 (1) (2012) 40–49.
[33] C. Hajiyev, H.E. Soken, Robust estimation of UAV dynamics in presence of measurement faults, J. Aerosp. Eng. 25 (1) (2012) 80–89.
[34] H.E. Soken, C. Hajiyev, S. Sakai, Robust Kalman filtering for small satellite attitude estimation in the presence of measurement faults, Eur. J. Control 20 (2) (2014) 64–72.
[35] S. Gao, G. Hu, Y. Zhong, Windowing and random weighting-based adaptive unscented Kalman filter, Int. J. Adapt. Control Signal Process. 29 (2) (2015) 201–223.
[36] W.L. Li, Y.M. Jia, J.P. Du, Windowing-based adaptive unscented Kalman filter for spacecraft relative navigation, in: Proceedings of the 34th Chinese Control Conference, Hangzhou, China, Jul. 28–30, 2015.
[37] C. Hajiyev, H.E. Soken, Adaptive fading UKF with Q-adaptation: application to picosatellite attitude estimation, J. Aerosp. Eng. 26 (3) (2013) 628–636.
[38] C. Hajiyev, H.E. Soken, Robust adaptive unscented Kalman filter for attitude estimation of pico satellites, Int. J. Adapt. Control Signal Process. 28 (2) (2014) 107–120.
[39] H.E. Soken, C. Hacizade, S. Sakai, Simultaneous adaptation of the process and measurement noise covariances for the UKF applied to nanosatellite attitude estimation, in: The 19th World Congress International Federation of Automatic Control, Cape Town, South Africa, Aug. 24–29, 2014, pp. 5921–5926.
[40] Y. Wang, S. Sun, L. Li, Adaptively robust unscented Kalman filter for tracking a maneuvering vehicle, J. Guid. Control Dyn. 37 (5) (2014) 1696–1701.
[41] J.H. Yoon, D.Y. Kim, V. Shin, Window length selection in linear receding horizon filtering, in: International Conference on Control, Automation and Systems, COEX, Seoul, Korea, Oct. 14–17, 2008, pp. 2463–2467.
[42] P.J. Huber, Robust Statistics, Wiley, New York, 1981.
[43] C. Hide, T. Moore, M. Smith, Adaptive Kalman filtering algorithms for integrating GPS and low cost INS, in: Position Location and Navigation Symposium, 2004, pp. 227–233.
[44] K. Baek, H. Bang, Adaptive sparse grid quadrature filter for spacecraft relative navigation, Acta Astronaut. 87 (2013) 96–106.
[45] G. Hewer, R. Martin, J. Zeh, Robust preprocessing for Kalman filtering of glint noise, IEEE Trans. Aerosp. Electron. Syst. 23 (1) (1987) 120–128.
[46] W.R. Wu, Maximum likelihood identification of glint noise, IEEE Trans. Aerosp. Electron. Syst. 32 (1) (1996) 41–51.
[47] E.M. Berti, A.J.S. Salmeron, F. Benimeli, Kalman filter for tracking robotic arms using low cost 3D vision systems, in: The Fifth International Conference on Advances in Computer–Human Interactions, Valencia, Spain, Jan. 30–Feb. 4, 2012, pp. 236–240.
[48] G. Bradski, A. Kaebler, Learning OpenCV, O'Reilly Media, 2008.
[49] S. Bruno, K. Oussama, Springer Handbook of Robotics, Springer-Verlag, Berlin and Heidelberg, 2008.

Wenling Li received his B.S. and M.S. degrees both in applied mathematics from Ocean University of China (OUC), Qingdao, China, in 2005 and 2008, respectively. He received his Ph.D. degree at Beihang University (BUAA), Beijing, China, in 2012. He is currently with the Seventh Research Division and School of Automation Science and Electrical Engineering at Beihang University. His research interests include Bayesian estimation, multi-target tracking and information fusion.

Shihao Sun received his B.S. degrees in applied mathematics from Beihang University of China (BUAA), Beijing, China, in 2010. He is currently working towards his Ph.D. degree in applied mathematics at the Seventh Research Division at Beihang University. His research interests include visual servo and robot control.

Yingmin Jia received his B.S. in control theory from Shandong University, Ji'nan, China, in January 1982, and his M.S. and Ph.D. both in control theory and applications from Beihang University (BUAA), Beijing, China, in 1990 and 1993, respectively. In 1993, he joined the Seventh Research Division at Beihang University, where he is currently a Professor of automatic control. His current research interests include robust control, adaptive control and intelligent control, and their applications in industrial processes and vehicle systems.

Junping Du received her Ph.D. in computer science from University of Science and Technology Beijing (USTB), and then held a postdoc fellowship with the Department of Computer Science at Tsinghua University, Beijing, China. She joined the School of Computer Science at Beijing University of Posts and Telecommunications (BUPT) in July 2006, where she is currently a Professor in computer science. Her current research interests include artificial intelligence, data mining, and intelligent management system development and computer applications.